Article:
Ruiz, JF, Soares, PJ, Alves Costa, P et al. (1 more author) (2019) The effect of tunnel construction on future underground railway vibrations. Soil Dynamics and Earthquake Engineering, 125. 105756. ISSN 0267-7261

https://doi.org/10.1016/j.soildyn.2019.105756

The Effect Of Tunnel Construction On Future Underground Railway vibrations

Jesús Fernández Ruiz [1], Paulo Jorge Soares[2], Pedro Alves Costa [2,4], David P. Connolly[3]

[1] University of La Coruña, Department of Civil Engineering, Campus de Elviña, 15071 La Coruña (Spain)
[2] University of Porto, Faculty of Engineering, Rúa Dr. Roberto Frías, s/n 4200-465 Porto (Portugal)
[3]Institute for High Speed Rail and Systems Integration, School of Civil Engineering, University of Leeds, UK

[4] Visiting Cheney Fellow, Institute for High Speed Rail and Systems Integration, School of Civil Engineering, University of Leeds, UK

Abstract.
This paper investigates the effect of initial tunnel construction on the future ground vibration levels generated during underground railway line operation. This is important because tunnel construction results in soil disturbance, thus inducing high strain levels in the soil near the tunnel lining. The resulting loss in soil stiffness can affect the future generation of ground-borne traffic vibration and it's propagation into the foundations of nearby buildings. To investigate this a hybrid modelling approach is developed, consisting of a construction simulation model and an elastodynamics model. First the convergence-confinement method is used to determine the stress state induced during tunnel construction using a tunnel boring machine (TBM). Next a 2.5D FEM-PML model consisting of vehicle-track-tunnel-soil is used to predict the vibration fields induced by underground trains. To link the approaches, the soil stiffness degradation contours computed from the tunnelling simulation act as inputs for the 2.5D underground railway model. This facilitates the assessment of the effect of tunnel construction on vibration levels. It is found that railway ground-borne vibration levels are underestimated if construction effects are ignored, with discrepancies of up to 10dB found at higher frequencies. Therefore, when estimating future vibration levels during the underground railway design stage (e.g. for subway, metro, high-speed lines…etc), tunnel construction should be considered as an operational source of uncertainty.

Keywords: Railway ground-borne vibration; Soil stiffness degradation; Underground railway tunnels; Vibration prediction uncertainty; Convergence-confinement tunnel modelling; 2.5D FEM-PML tunnel modelling; Soil non-linearity; Tunnel boring machine modelling

1. INTRODUCTION

Underground railways generate vibrations during train passage which may propagate to nearby structural foundations, causing vibrations and re-radiated noise in buildings. This disturbs inhabitants and sometimes can make buildings unusable for their intended purpose. Therefore numerical models are commonly used to predict this vibration generation and propagation. These models typically ignore the effect of the mechanical tunnelling processes performed during construction on the soil properties in the vicinity of the tunnel. This is important because large strains are permanently induced at this location. Considering railway vibration generation and propagation is highly dependent

upon soil stiffness, this means tunnel construction methods can play a role on the future ground-borne vibration levels when trains operate in the tunnel.

To model the ground vibrations induced due to underground railways (in absence of tunnelling process effects), a variety of semi-analytical approaches have been proposed. These include: Hussein and Hunt [1], Kuo, Hunt and Hussein [2],Müller [3] , He, Zhou, Di, Guo and Xiao [4], Yuan, Boström and Cai [5], Yuan, Cai and Cao [6], Hussein, François, Schevenels, Hunt, Talbot and Degrande [7]. The main advantage of these type of approaches is their high computational efficiency. However this efficiency compromises versatility (e.g. only limited geometries can be simulated) meaning they are difficult to use in engineering practice.

An alternative approach is to use numerical models. These offer greater versatility but require the solving of large systems of equations due to the 3D nature of the problem and broadband spectra of frequency contents. Therefore they often require large computational effort to solve. To minimise this though, it can be assumed that the domain is invariant or periodic in the train passage direction, thus facilitating the use of transformed domain techniques that reduce computational effort.

If the problem cross-section is assumed invariant, the so-called 2.5D technique is used in order to obtain the 3D response of the problem in an efficient manner [8]. This concept has been explored using the finite element method (FEM) [9-11], the boundary element method [12-14], and the Method of Fundamental Solutions (MFS) [15]. If the problem requires the simulation of complex geometries, FEM is typically the preferred method. However, it requires coupling with an absorbing condition to prevent spurious reflections contaminating the solution. This can be done by coupling with an alternative modelling approach [13-17] such as the boundary element method. Alternatively, rather than use multiple different approaches, an absorbing boundary condition can be used purely within the FE approach. This can be achieved using several techniques, including: infinite elements [8, 18], viscous absorbing boundaries [19, 20], scaled boundary finite elements [21] and perfectly matched layers [22, 23]. As an example, [23-25] [26] showed that it is possible to achieve high accuracy 3D solutions using the 2.5D FEM-PML approach without losing computational efficiency.

As an alternative to assuming the problem is invariant, it can also be considered periodic. This is particularly useful for ballasted tracks. For example, if each repeated sleeper bay geometry is periodic, then a Floquet transformation (Clouteau, Arnst, Al-Hussaini and Degrande [27]) can be used to recover the full 3D response for an infinite number of sleeper bays, from only a single sleeper bay. This has been used intensively used by Gupta et al. [28-32] for the study of vibrations induced by railway traffic in tunnels.

The aforementioned approaches have led to a deeper understanding of the underground railway vibration problem [23, 25, 28, 31]. To validate these numerical models, experimental data has been used [17, 24, 30], however often there are discrepancies between the predicted and measured responses. These have been attributed to the lack of information about system properties or other sources of uncertainty [33, 34]. However some assumptions of the models proposed to-date, include that the material behaviour is elastic, linear and the same as found during the geotechnical investigation made prior to tunnel construction.

The assumption of linear elastic behaviour is reasonable because train loads induce very small strains (10^{-6}-10^{-5}) in the soil, particularly for tunnel arrangements. However, during tunnel drilling and lining construction, much larger strains (in the range of 10^{-4}-10^{-2}) are induced in the soil [35]. In this range, soil behaviour is not elastic, and is characterized by an irreversible degradation of shear stiffness. This depends on several

factors, including: tunnel diameter, tunnel perforation method, tunnel depth and nature of the soil. This loss of stiffness is not equal at all soil locations affected by the tunnelling process, and is instead more pronounced in the tunnel vicinity, where shear strains are dominant. Therefore the soil shear modulus post-construction in the tunnel vicinity is different to the at-rest conditions prior to construction. This was investigated by Gomes [36] where it was shown that construction induced stiffness degradation plays an important role on tunnel seismic response. However, to the authors' knowledge, there are no studies investigating the effect on tunnel construction activities on railway tunnels vibrations. Therefore this paper investigates this. First a numerical model is presented to simulate the tunnel construction process undertaken by a tunnel boring machine. It is used to compute the stiffness degradation in the soil surrounding the tunnel. These degraded soil properties are then used as inputs for a separate railway tunnel vibration prediction model. This 2.5D model is used to predict ground-borne vibration levels at the ground surface in the presence of stiffness degradation. The results are compared against the assumption of ignoring degradation.

2. METHODOLOGY

2.1 Overview

The numerical approach adopted in this paper uses 2 separate, yet linked, numerical models as shown in Figure 1. First, tunnel construction is simulated through a model developed using the commercial software, PLAXIS. This is used to compute the shear stiffness (G) degradation of the soil in the vicinity of the tunnel lining. Then, using the modified soil stiffness profile distribution due to tunnelling, a wavenumber/frequency domain 2.5D FEM-PML model is used to predict the ground vibrations induced by railway traffic. The overall modelling solution is therefore able to assess the effect of tunnelling on the generation and propagation of ground vibration. Figure 1 depicts the main steps of the proposed approach:

1) Tunnel construction is simulated in PLAXIS, using a non-linear soil model, and stiffness degradation maps are generated
2) The 3D dynamic response of the track-tunnel-ground system is computed taking into account the stiffness degradation computed in step 1
3) The train-track dynamic interaction problem is solved
4) The dynamic loads applied by the train to the track are used to compute the vibrations in the track-tunnel-ground system

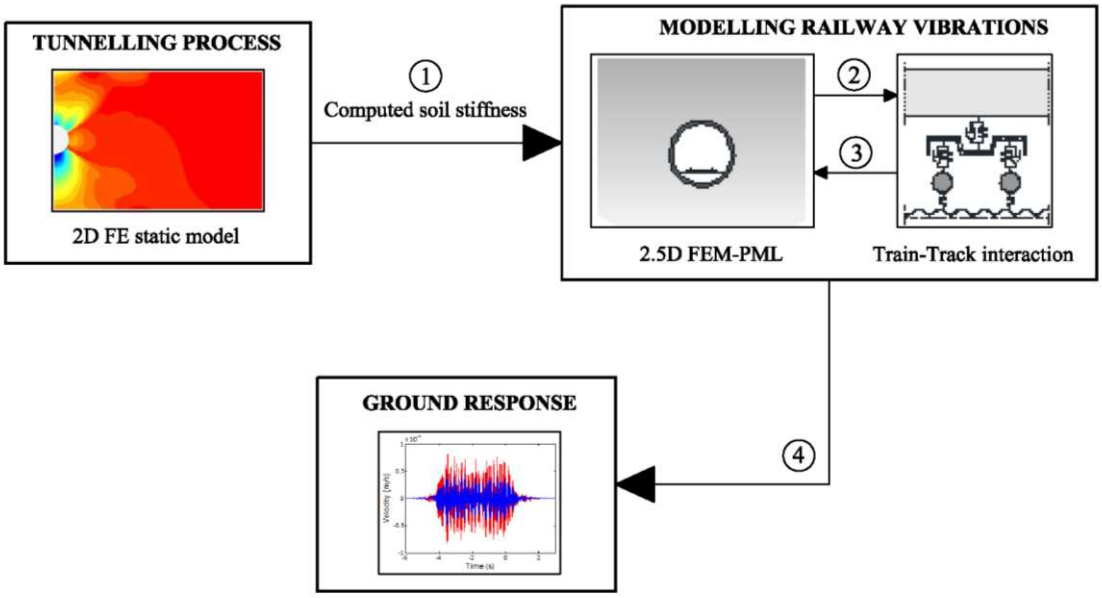

Figure 1. Schematic of the global sub-structure modelling approach.

2.2 Tunnelling process modelling

The aim of the tunnelling modelling is to generate a shear stiffness (G) map of the soil domain. However, the mechanical behaviour of soil is complex, requiring the accurate simulation of response from very small strains to large strains range. This challenge has been scope of numerous research projects, resulting in a variety of proposed approaches, including: Hyperbolic models [37], Hardening soil models [38] and Hardening soil models with small-strain stiffness [39], among others. The latter is used in this study since the Hardening Soil model with small-strain stiffness (HSsmall) is an extension of the Hardening Soil model. This model uses the Mohr-Coulomb failure criterion and is able to reproduce both shear and compression soil hardening though hyperbolic laws combined with the classical theory of plasticity. Unloading and reloading conditions are assumed as elastic responses and the broad strain range, from very small strains (elastic behaviour) to large strains (non-linear behaviour) is considered using straightforward hyperbolic laws [40].

To simulate the tunnel construction, the convergence-confinement method (CCM) using plane strain finite elements method is used. Although tunnel construction is a three dimensional problem, Panet and Guenot [41] demonstrated that 3D ground response can be approximated using a 2D plane strain numerical approach if careful assumptions are made. The basis of this method is to provide a fictitious pressure inside the 2D tunnel model to account for the arching effect that occurs within the surrounding soil due to the close proximity of the tunnel face. This effect disappears when the tunnel face is far from the section under consideration, as depicted in **Figure 2**. The fictitious pressure, σ_r^f, is calculated from the initial stress in the ground (σ_r^0) and the stress release coefficient (β) as:

$$\sigma_r^f = (1-\beta)\sigma_r^0 \quad (1)$$

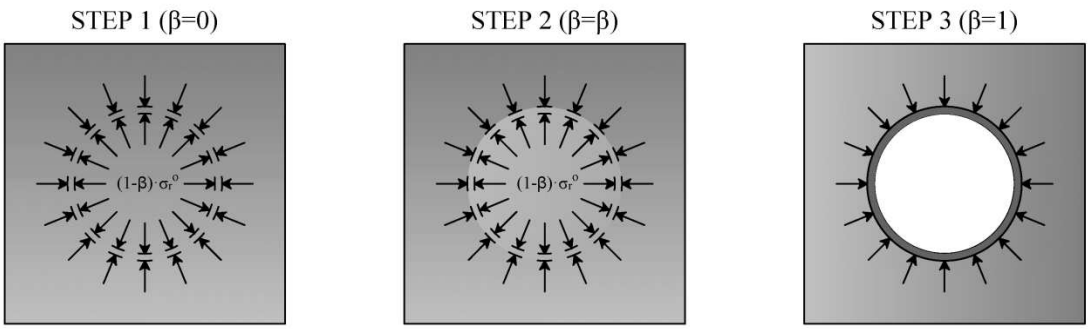

Figure 2. Schematic of the convergence-confinement method for tunnel construction simulation.

The stress release coefficient can be estimated through 2D and 3D numerical comparisons or even through experimental measurements, although these are scarce in the literature [42-45]. It typically lies between 0.2-0.8 depending on: excavation method, tunnel diameter, overburden pressure, soil type among other factors.

The tunnelling simulation procedure involves 3 main steps as shown in **Figure 2**:

- Step 1: the initial effective stress field is generated using gravity loading via a prescribed K_0-value. In the tunnel boundary, the external earth pressure (σ_r^0) and internal pressure (σ_r^f) are identical, which means that $\beta=0$.
- Step 2: the stress-strain field is computed in the cross section located between the tunnel face and the lining, with arching effect simulated using the stress release coefficient. The internal pressure is given by equation 1, where β is the stress release coefficient.
- Step 3: lining is installed and the stress-strain field is computed assuming a permanent condition, i.e., assuming that the tunnel face is far away from the section under analysis. In such case $\beta=1$, which means that fictitious pressure is not acting anymore.

2.3 Railway traffic vibration modelling

The simulation of traffic induced vibrations is complex due to a variety of factors, including, obviously, the train-track dynamic interaction, which is governed by: i) the track unevenness, ii) the lack of roundness of the wheels, iii) non-homogeneous support conditions, among other factors. These heterogeneities cause dynamic forces in the train, and therefore, train-track dynamic interaction loads vary with time. To simulate these complexities, a sub-structuring approach is used. Figure 3 shows a schematic representation of the different sub-models that are used to predict the final railway vibration levels. The elastic 2.5D FEM-PML method is used for the track-tunnel-ground system, while a multibody approach is used for the vehicle. The reader can find a comprehensive description of the modelling details in previous papers by the authors [23-25].

Regarding excitation, the quasi-static and dynamic excitation mechanisms are uncoupled, with the final solution obtained using by superposition of both effects. Furthermore, only the dynamic excitation mechanism due to the track irregularities is taken into account. The following equation is used to address the PSD (power spectral density of unevenness amplitude) of the track unevenness:

$$S(k_1) = S(k_{1,0})\left(\frac{k_1}{k_{1,0}}\right)^{-w} \quad (1)$$

Regarding soil properties, the vibration model uses the information provided by the tunnelling model to determine the soil stiffness at each location. Therefore the element-by-element stiffness's from the tunnelling mesh are converted to the vibration mesh through 2D interpolation. It should be noted that the tunnelling model does not allow for changes in the soils Poissons' ratio, soil density or damping. Therefore they are constant for all vibration simulations.

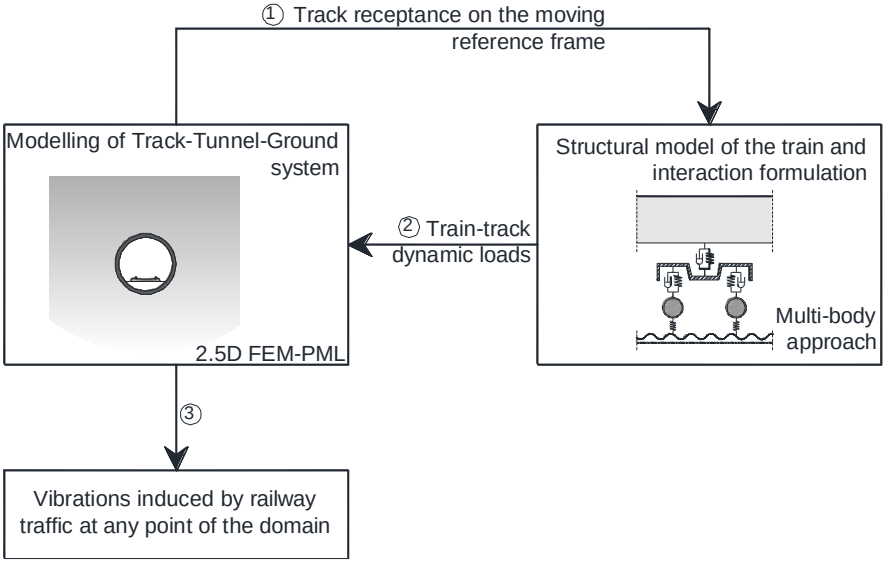

Figure 3. Schematic of the model used for predicting railway traffic vibrations

3. CASE STUDY

3.1. Tunnelling input properties

The tunnel and soil input characteristics are informed by properties measured experimentally during the construction of the Porto metro network in Portugal. The geometry of the finite element mesh used to simulate the tunnel construction is shown in Figure 4. The tunnel crown depth is 15m below the ground surface which is consistent with tunnels commonly constructed using tunnel boring machines. The tunnel has a lining thickness, e, of 0.35 m, formed from reinforced concrete with the following properties: volumetric mass equal to 2500 kg/m^3, Young modulus equal to 30 GPa and Poisson's ratio equal to 0.2.

Regarding the soil, it is a homogenous granite residual soil, with the properties outlined in Topa Gomes [46], and expanded upon in Table 1. The low-strain shear modulus $G_{0,}$ (and consequently E_0) and the unloading shear stiffness G_{ur} (E_{ur}), were determined using cross-hole tests and pressumeter tests respectively. Further, triaxial tests were used to determine E_{50} (secant Young modulus for stress level corresponding to 50% of the shear strength), the friction angle, φ', and the coesion, c'. Oedeometer tests were performed to determine Young modulus, E_{oed},, coefficient m has been considered null and the value of 0.3 was assumed for the Poisson ratio (ν). The at-rest coefficient is defined as K_0, and the dilatancy angle as ψ.

Considering the uncertainties around the stress release coefficient, two values are tested: 0.5 and 0.4, values which are consistent for residual soils bored using a TBM (Tunnel Boring Machine), which usually induce small deformations in the ground.

Table 1 : Parameters adopted for HSsmall constitutive model

γ_{ap} (kN/m^3)	20	Ψ	5^o
E_{50}^{ref} (kN/m^2)	$97.5 \cdot 10^3$	v'	0.3
E_{oed}^{ref} (kN/m^2)	$121.9 \cdot 10^3$	K_o^{nc}	0.5
E_{ur}^{ref} (kN/m^2)	$195 \cdot 10^3$	$\gamma_{0.7}$	$3.5 \cdot 10^{-4}$
m	0	G_0^{ref} (kN/m^2)	$150 \cdot 10^3$
c' (kN/m^2)	30	p_{ref} (kN/m^2)	100
φ'	40^o	R_f	0.9

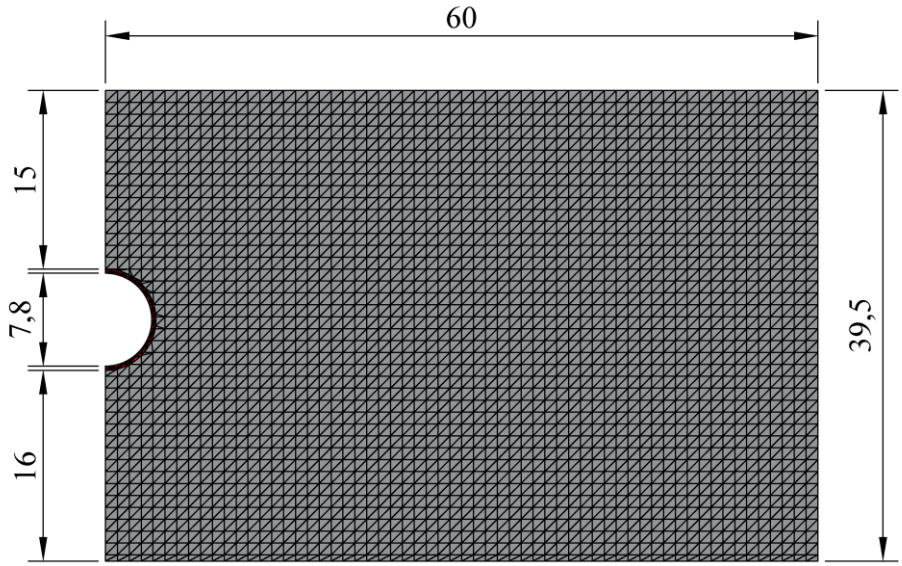

Figure 4. Finite elements mesh used for tunnel construction process simulation [m].

The curves γ_s-G_s and γ_s-G_t of this soil constitutive model are shown in Figure 5.

For the vibration analysis, the value adopted for the linear shear modulus (G) is the largest between G_s and G_t. Since the strains induced by construction are distinct for different locations in the tunnel vicinity and therefore also different are the stiffness degradation levels, it results that the vibration analysis is performed assuming different elastic properties in each finite element.

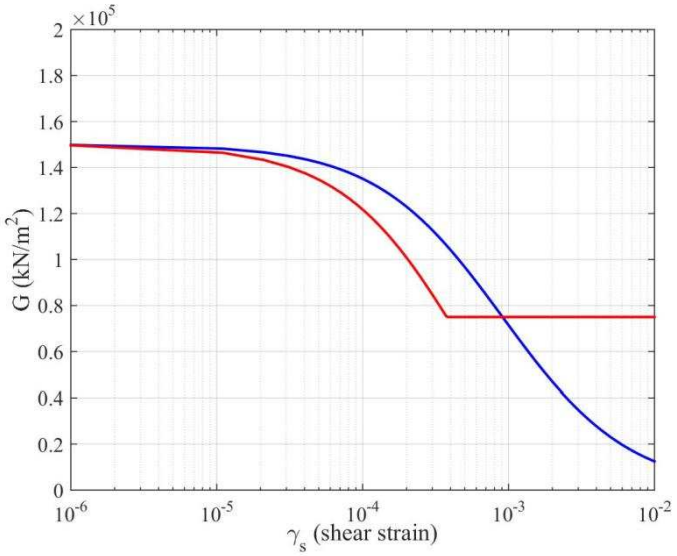

Figure 5. Curves of γ_s-G_s (blue line) and γ_s-G_t (red line) in HSsmall model.

3.2. Railway vibration input properties

The soil properties of the tunnel post-construction are computed using the tunnelling model and then used as input data for the railway vibration model. For all scenarios the soil density is 2000 kg/m^3, the Poisson ratio is 0.3 and the hysteretic damping ratio is 0.04. To quantify the effect of different tunnelling procedures, three sets of analysis are undertaken:

1. Neglecting all soil stiffness degradation effects induced during tunnelling;
2. Accounting for soil stiffness degradation effects induced during tunnelling, using a release factor of 0.4;
3. Accounting for soil stiffness degradation effects induced during tunnelling, using a release factor of 0.5;

Figure 6 shows the railway tunnel vibration mesh used for computations. Regarding the railway track properties, it is a continuous concrete slab track 0.3 m thick and 2.5 m wide, with a longitudinal bending stiffness of 1.62×10^8 N/m^2 and a mass of 3000 kg per unit of length. The rails are UIC60 profile, and are continuously supported by railpads with a stiffness and damping coefficients of 5×10^8 N/m^2 and 1.2×10^5 Ns/m^2 respectively. The track is a floating slab, with a resilient mat located between the slab and tunnel invert. It has a stiffness of 1.53×10^8 N/m^2 per meter in the longitudinal direction, and a damping of 5.5×10^4 Ns/m^2. The track unevenness is artificially generated for a range of wavelengths between 28 m and 0.55 m. The PSD curve adopted in this random generation is given by equation 1 where: $k_{1,0}$=1 rad/s, w=3.5 and $S(k_{1,0}) = 1 \times 10^{-8}$ m^3.

Regarding rolling stock, it is an Alfa-Pendular train at a running speed of 40 m/s. The main geometrical and mechanical properties of the train are summarized in Figure 7 and in Table 2.

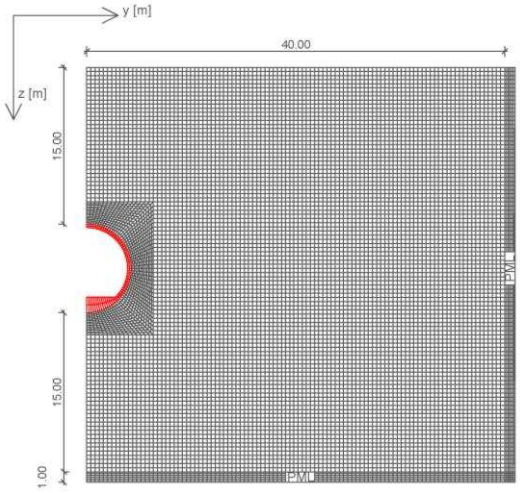

Figure 6. 2.5D finite elements mesh used for the ground-borne vibration analysis.

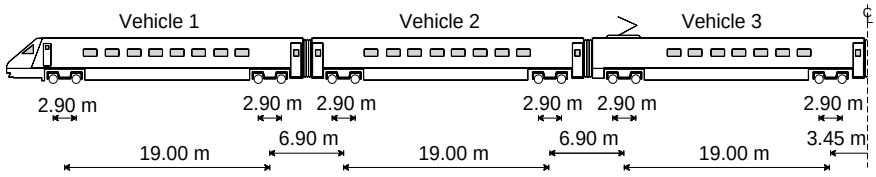

Figure 7. Alfa-Pendular geometry.

Table 2 : Mechanical properties of the Alfa-Pendular train

Axles	**Mw (kg)**	**1538-1884**
Primary suspension	**Kp (kN/m)**	**3420**
	Cp (kNs/m)	**36**
Bogies	**Mb (kg)**	**4712-4932**
	Jb (kg/m^2)	**5000-5150**
Car body	**Mc (kg)**	**32900-35710**

4. RESULTS AND DISCUSSION

4.1. Soil stiffness degradation due to tunnel construction

Figure 8 shows G/G_0 contour plots resulting from tunnel construction for the release factors of 0.5 and 0.4. It can be observed that the stiffness degradation is more relevant in the points closest to the tunnel, and in some places, drops to as low as G/G_0=0.6. A small amount of degradation propagates to the soil surface, however, the stiffness degradation effect is limited to a maximum lateral distance of approximately 25 to 30 meters from the tunnel centre-line. The stiffness degradation is larger for the higher release factor, because this means that the soil is less confined before tunnel lining installation. Although there are some discrepancies, in general the stiffness degradation pattern is similar for both scenarios.

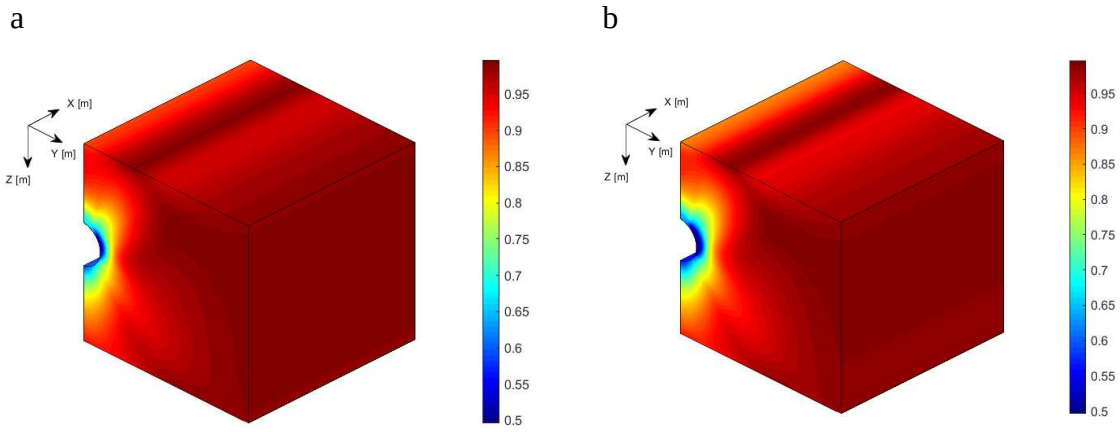

Figure 8. G/G_0 Stiffness contours due to tunnelling, (a) $\beta = 0.4$, (b) $\beta = 0.5$

4.2. The effect of soil degradation on post-construction railway vibration propagation

4.2.1 Transfer functions for stationary loads

The practical assessment of railway ground vibrations often relies on determining the in-situ transfer function between tunnel invert and surface [47, 48]. Therefore this section aims to replicate a similar scenario to determine the effect of soil stiffness degradation on vertical particle velocity transfer functions assessed from the tunnel invert to the ground surface. To do so, a stationary unitary harmonic load is applied at the tunnel invert and the response recorded at 6 locations on the soil surface (Figure 9). The test is repeated for the 3 cases discussed above: no degradation, degradation release factor 0.4, and degradation release factor 0.5.

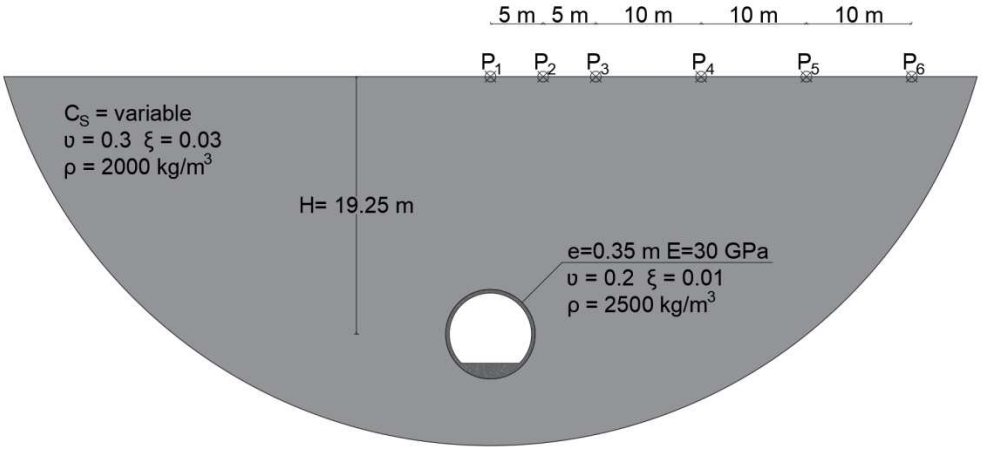

Figure 9. Location of ground vibration receivers

Figure 10 compares the vertical velocity transfer function of all output locations, with varying input load frequency. The numerous distinct lobes show that the dynamic response of the ground surface is complex. This is due to the interaction of shear, compression and Rayleigh waves. It is also dependent on the distance between source-receiver and on the elastic soil properties, as shown by Gupta et al. [28]. Considering the three stiffness degradation scenarios, the following conclusions are drawn:

1. For all the receivers there is a range of low frequencies for which the three transfer functions are almost identical. This range varies from 0 Hz to a frequency that is depending on receiver location.
    - For points 0, 5 and 10 meters, it is approximately 12 Hz
    - For points located 20 and 30 meters far away from the tunnel centre line, it is approximately 20 Hz
    - For the P6 point (40m far away from tunnel centre line), it is 27 Hz

    This is because lower frequencies give rise to longer wavelengths and, consequently, are not so strongly affected by the stiffness variations located in the immediate vicinity of the tunnel. This frequency grows with the increase in distance from the tunnel because the degradation of stiffness along the wave propagation path is less relevant for the points located further away from the tunnel, as can be seen in Figure 10.

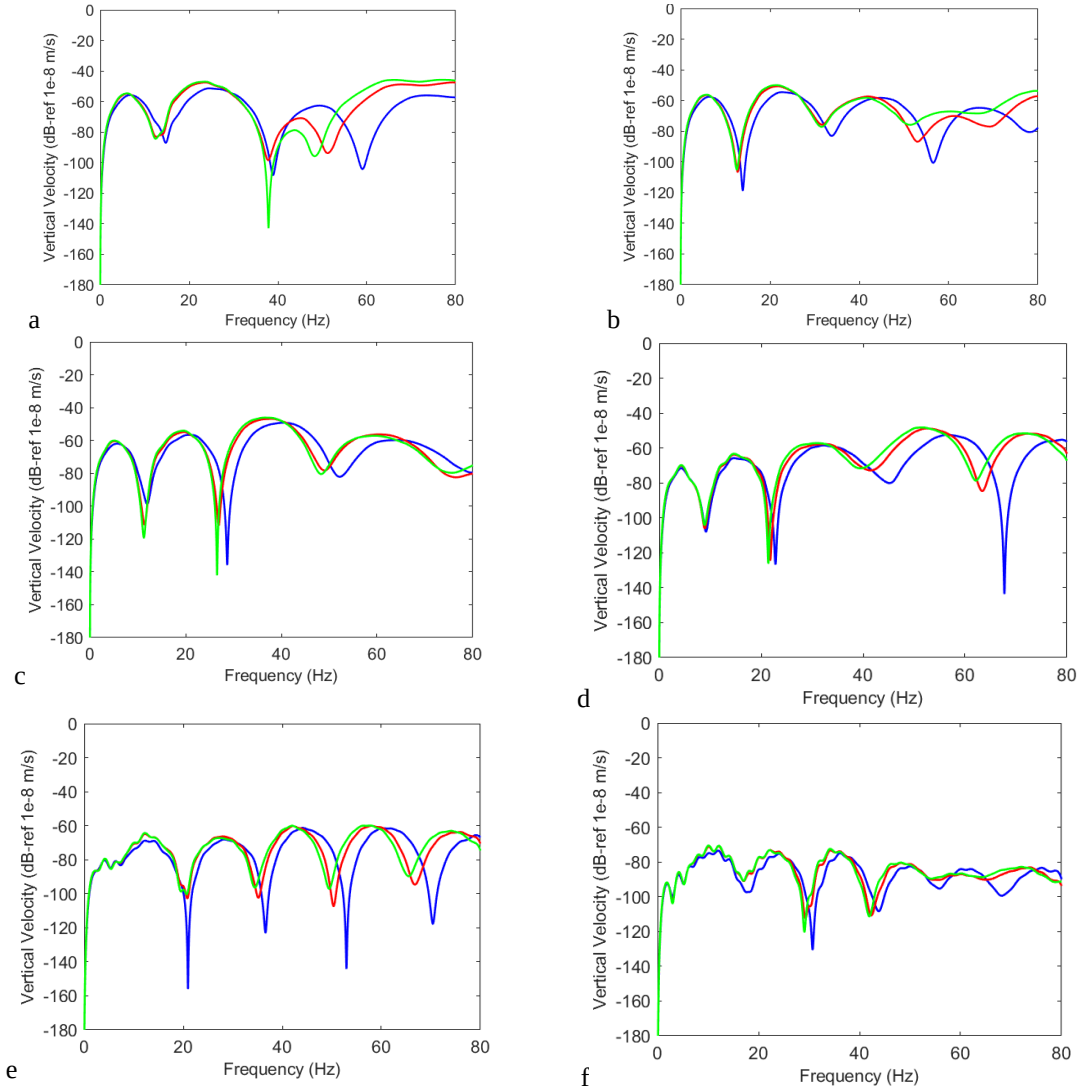

Figure 10. Vertical velocity transfer functions due to a load applied at the tunnel invert and evaluated at the ground surface: a) P1; b) P2; c) P3; d) P4; e) P5; f) P6 (blue line: non disturbed soil; red line: disturbed soil $\beta = 0.4$; green line: disturbed soil $\beta = 0.5$)

2. As distance from the tunnel increases, the discrepancies between the three transfer functions decreases. At distances greater than 30 meters the discrepancies become irrelevant in the frequency range up to 50 Hz.
3. The transfer functions troughs shift to lower frequencies when stiffness degradation is taken into account. When the ground stiffness is lower, the frequencies at which the troughs occur are lowered, particularly when the source-receiver distance is short. For the point located at 40 m away from the tunnel alignment, the change in trough frequencies is negligible because at this distance the global system response is governed by the undisturbed ground properties;
4. Comparing results from release factor of 0.4 and 0.5, it is possible to observe differences in the frequency range above 50 Hz mainly for the points located close to the tunnel symmetric plane. As expected, amplitude of vertical velocity increases with degree of soil disturbance(i.e. larger values of β.) This effect is quite evident in Figure 10a and Figure 10b.

4.3. Vibrations due to railway traffic

This section analyses the track-tunnel-ground system response when excited by the passage of an Alfa-Pendular train running at a speed of 40 m/s. Figure 11 shows the dynamic response of the track slab in terms of vertical particle velocity. As expected, the time record shown in Figure 11a allows for the identification of the passage of each train axle. Comparing the vertical velocity time record for the three scenarios under study, it is seen that the peak velocity is just slightly affected by the soil disturbance induced by tunnelling operations. Actually, this is an expected result since the dynamic response of the track in tunnels is mainly governed by the elastic properties of the resilient elements that are much softer than the foundation. This effect is also evident using frequency domain analysis in Figure 11b, which shows the equivalent response in terms of one-third octave bands. Comparing the spectrum for the 3 cases, it is interesting to observe that the dynamic response for a release factor of 0.4 or 0.5 is almost equal to the dynamic response obtained when the soil disturbance is neglected. However, a more detailed analysis allow to see that in the frequency range around 50 Hz there is an amplification of approximately 4 dB in the response when stiffness degradation due to tunnel construction is taken into account.

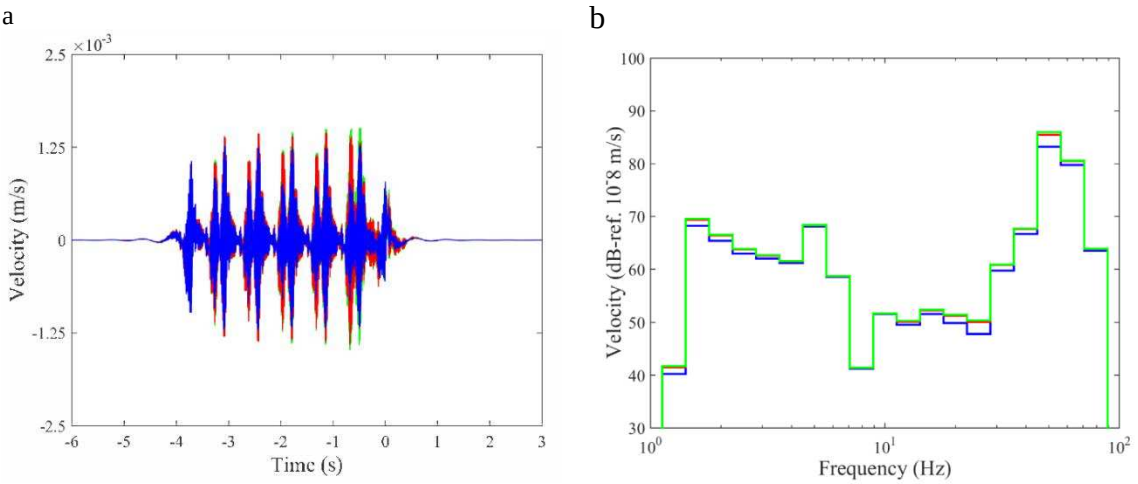

Figure 11. Vertical velocity in slab (blue line: non disturbed soil; red line: disturbed soil β = 0.4; green line: disturbed soil β = 0.5): a) time record; b) one-third octave frequency spectrum.

The analysis of the dynamic response at surface receiver locations is important from an environmental perspective because these are where building foundations are most likely to be located. Therefore the vibrations induced by traffic in tunnels may cause building vibration and re-radiated noise at these locations.

Figure 12 shows time-records of vertical velocity due to the passage of the Alpha Pendular train, at the receiver points indicated in Figure 9. For the cases where tunnelling has reduced the soil stiffness, the vibrations are much larger, indicating that ignoring construction effects serves to underestimate vibration levels. This effect is pronounced at locations in close proximity to the tunnel lining, where large differences on peak particle velocity are observed, and reduces with distance. At a lateral offset of 40m, the discrepancy becomes negligible.

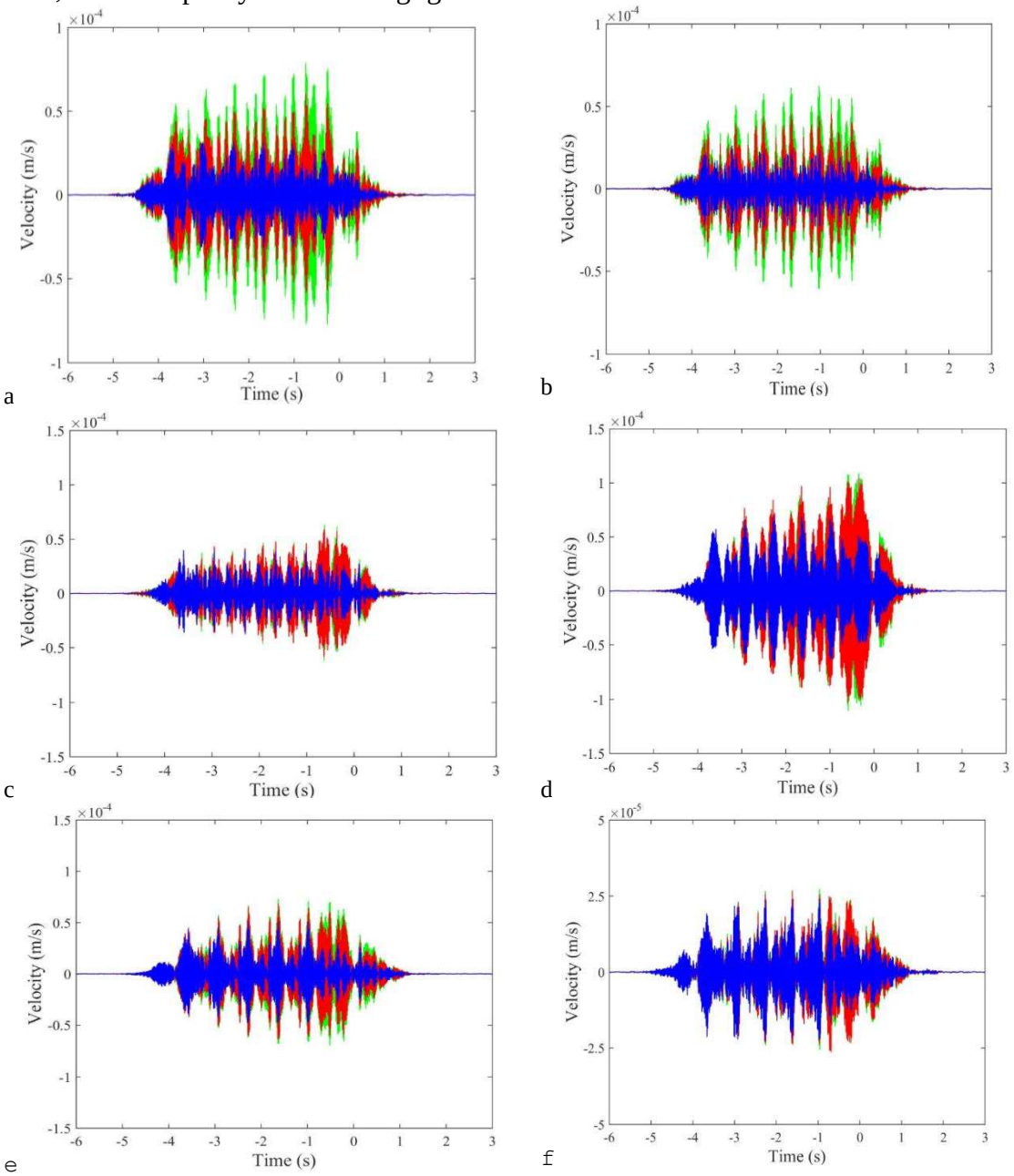

Figure 12. Time records of vertical velocity at the ground surface: a) P; b) P2; c) P3; d) P4; e) P5; f) P6 (blue line: non disturbed soil; red line: disturbed soil $\beta = 0.4$; green line: disturbed soil $\beta = 0.5$)

Figure 13 shows the same results as Figure 12, but presented in one-third band octave spectra, to allow for a more detailed analysis of the frequency content. Consistent with Figure 12, all cases yield high levels of ground vibration when stiffness degradation is considered. This is true mainly in the frequency range between 40 Hz to 60 Hz, where discrepancies of up to 10dB are identified. Although all receiver locations experience this, in the same manner as the time history results, the largest discrepancies occur at the locations close to the tunnel and diminish with distance.

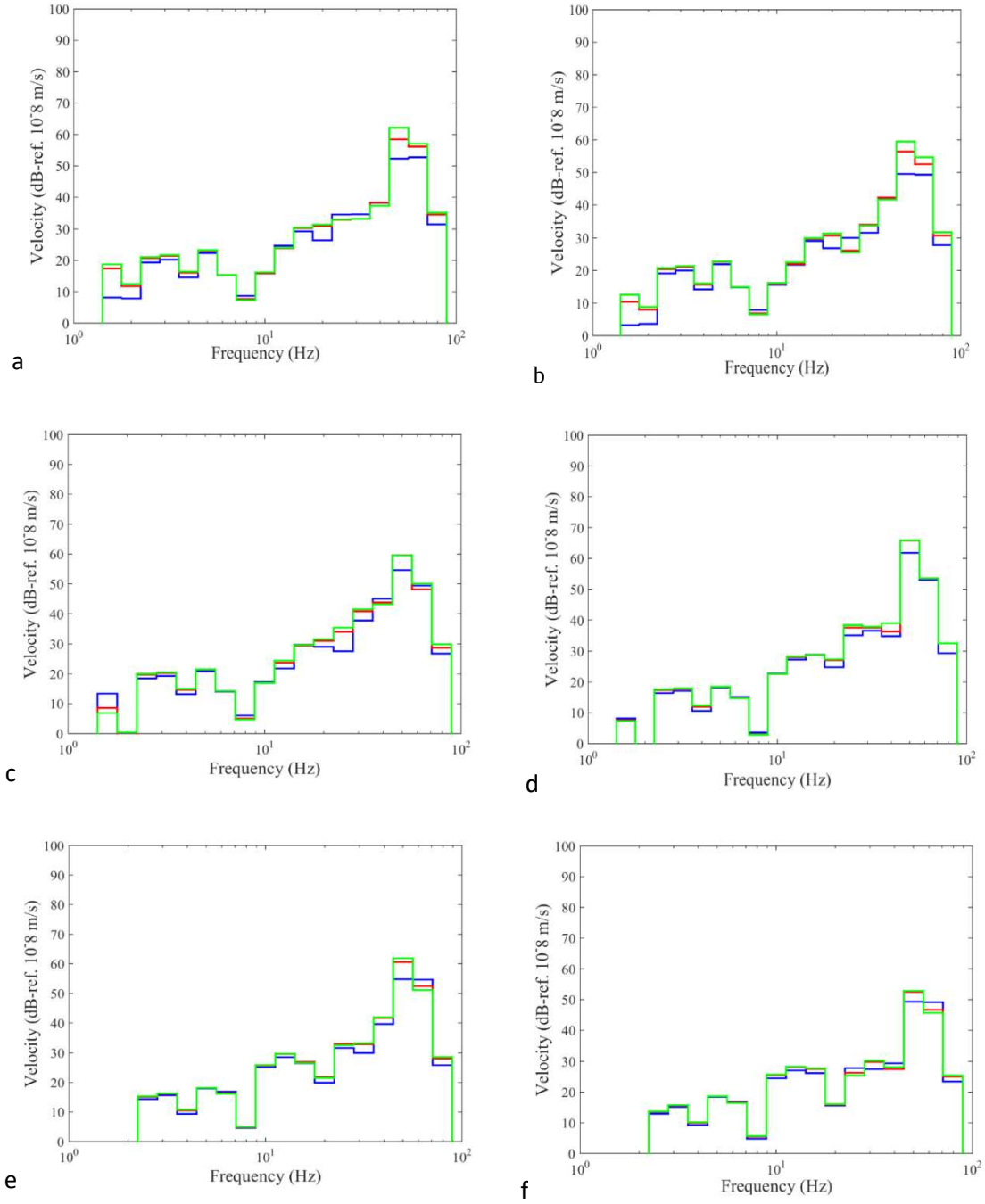

Figure 13 . One-third octave spectrums of vertical velocity at the ground surface: a) P1; b) P2; c) P3; d) P4; e) P5; f) P6 (blue line: non disturbed soil; red line: disturbed soil $\beta = 0.4$; green line: disturbed soil $\beta = 0.5$)

Independent of the release factor, comparing the results where tunnelling construction was considered with the case where construction stage was not taken into account, the velocity differences at frequencies below 20 Hz are limited when the receiver is located more than 15 m from the tunnel centre line. However, above this frequency value, the differences are evident in all the points analysed, reaching up to 10 dB at closest distances to the tunnel. These differences decrease with the increasing distance of the tunnel-receiver. For example, at points located 30 and 40 meters away from the axis of the tunnel, the discrepancy is minimal, except for the frequency band of 50 Hz where there are still significant differences. This is because at low frequencies the wavelengths are large and are less influenced by local changes in stiffness. In contrast, for high frequencies the wavelengths are short, thus causing them to be affected by local stiffness changes. It should however be noted that the analysis of wave propagation in the presence of stiffness degradation is quite complex, and there is not always a rational explanation for all discrepancies. However, in this case, the responses due to train passage agree with the stationary load transfer functions, which was previously explained.

Regarding release factor, comparing the cases of $\beta=0.4$ and $\beta=0.5$, a similar trend in octave frequencies is observed, with the highest level of vibrations, for all receivers, occurring in the frequency range 40-60 Hz. However, the $\beta=0.5$ case yields higher vibration levels than the $\beta=0.4$ case, and the case of zero degradation. This is an expected result because a greater release factor β indicates a greater degradation of soil properties during the tunnel construction process.

In conclusion, it is clear that the effect of soil stiffness degradation in the immediate vicinity of the tunnel results in elevated ground-borne vibration levels at the soil surface. This effect is prominent for the medium and high frequency range. Its magnitude is non-negligible and should be considered as a factor of uncertainty when designing vibration mitigations measures for railway tunnels.

5. CONCLUSIONS

In this paper the effects of soil stiffness degradation due to tunnelling operations, on the propagation of vibrations induced by underground railway traffic is studied. To investigate this a two-step approach is used consisting of a model to simulate tunnel construction, and an elastic 2.5D vibration model to simulate the generation and propagation of vibrations from trains. The results show that the effect of tunnel construction should be considered when assessing ground-borne vibration levels from future planned post-construction railway lines. More specifically, it is found that:

i) The influence of soil stiffness degradation on both free-field railway vibrations, and stationary transfer functions due to an impact excitation is important. Vibration levels can increase by up to 10dB if significant soil disturbance occurs during tunnel construction.

ii) Construction-induced soil stiffness degradation influences locations located close to the tunnel more than locations at large distance. For example, locations directly above the tunnel are affected most greatly, while locations at offsets greater than 30m yield similar results to when ignoring Construction-induced effects.

iii) Soil disturbance, and thus stiffness degradation, is primarily located in the immediate vicinity of the tunnel, and decreases with distance from the lining. Therefore it effects medium-high frequency wave propagation, rather than the low frequencies. In the example presented, only frequencies greater than 20Hz are effected by the construction process of the tunnel boring machine.

iv) Soil stiffness degradation has a small influence on the dynamic track response. It increases by approximately 4 dB when considering the effects of tunnelling.

Finally, it should be noted that the example presented is for a tunnel constructed using a tunnel boring machine through relatively stiff soil. The increase in vibration levels could be greater for tunnels constructed using open section methods (NATM) or through soft soils, where even higher ground strain levels are induced.

ACKNOLEDGMENTS

This research was financially supported by: Project POCI-01-0145-FEDER-007457–CONSTRUCT–Institute of R&D In Structures and Construction funded by FEDER funds through COMPETE2020– Programa Operacional Competitividade e Internacionalização (POCI)–and by national funds through FCT–Fundação para a Ciência e a Tecnologia;Project POCI-01-0145-FEDER-029577–funded by FEDER funds through COMPETE2020 – Programa Operacional Competitividade e Internacionalização (POCI) and by national funds (PIDDAC) through FCT.

The financial support provided by University of Leeds Cheney Award Scheme, the Leverhulme Trust (UK) and by the construction company "Arias Infraestructuras S.A." through FICG (Fundación Ingeniería Civil de Galicia) of the University of La Coruña are also appreciated.

6. REFERENCES

[1] Hussein, M. and H.E.M. Hunt, *A numerical model for calculating vibration from a railway tunnel embedded in a full-space*. Vol. 305. 2007. 401–431.

[2] Kuo, K., H. Hunt and M. Hussein, *The effect of a twin tunnel on the propagation of ground-borne vibration from an underground railway.* Journal of Sound Vibration, 2011. **330**(25): p. 6203-6222.

[3] Müller, K., *Dreidimensionale dynamische Tunnel-Halbraum-Interaktion*. 2007, Technische Universität München.

[4] He, C., S. Zhou, H. Di, P. Guo and J. Xiao, *Analytical method for calculation of ground vibration from a tunnel embedded in a multi-layered half-space.* Computers Geotechnics, 2018. **99**: p. 149-164.

[5] Yuan, Z., A. Boström and Y. Cai, *Benchmark solution for vibrations from a moving point source in a tunnel embedded in a half-space.* Journal of Sound and Vibration, 2017. **387**: p. 177-193.

[6] Yuan, Z., Y. Cai and Z. Cao, *An analytical model for vibration prediction of a tunnel embedded in a saturated full-space to a harmonic point load.* Soil Dynamics and Earthquake Engineering, 2016. **86**: p. 25-40.

[7] Hussein, M., S. François, M. Schevenels, H. Hunt, J. Talbot and G. Degrande, *The fictitious force method for efficient calculation of vibration from a tunnel embedded in a multi-layered half-space.* Journal of sound and vibration, 2014. **333**(25): p. 6996-7018.

[8] Yang, Y.B. and H.H. Hung, *A 2.5D finite/infinite element approach for modelling visco-elastic body subjected to moving loads.* International Journal for Numerical Methods in Engineering, 2001. **51**: p. 1317-1336.
[9] Lopes, P., P. Alves Costa, R. Calçada and A. Silva Cardoso, *Numerical Modeling of Vibrations Induced in Tunnels: A 2.5D FEM-PML Approach*, in *Traffic Induced Environmental Vibrations and Controls: Theory and Application*, H. Xia and R. Calçada, Editors. 2013, Nova. p. 133-166.
[10] Hung, H. and Y. Yang, *Analysis of ground vibrations due to underground trains by 2.5D finite/infinite element approach.* Earthquake Engineering and Engineering Vibration, 2010. **9**(3): p. 327-335.
[11] Bian, X., E. Zeng and Y. Chen, *Ground motions generated by harmonic loads moving in subway tunnel*, in *Proceedings of the Third International Symposium on Environmental Vibrations: Prediction, Monitoring, Mitigation and Evaluation. ISEV 2007*. 2007: Taipei, Taiwan.
[12] Rieckh, G., W. Kreuzer, H. Waubke and P. Balazs, *A 2.5D-Fourier-BEM model for vibrations in a tunnel running through layered anisotropic soil.* Engineering Analysis With Boundary Elements, 2012. **36**: p. 960-967.
[13] Ghangale, D., A. Colaço, P.A. Costa and R. Arcos, *A Methodology Based on Structural Finite Element Method-Boundary Element Method and Acoustic Boundary Element Method Models in 2.5D for the Prediction of Reradiated Noise in Railway-Induced Ground-Borne Vibration Problems.* Journal of Vibration and Acoustics, Transactions of the ASME, 2019. **141**(3).
[14] Galvín, P., S. François, M. Schevenels, E. Bongini, G. Degrande and G. Lombaert, *A 2.5D coupled FE-BE model for the prediction of railway induced vibrations.* Soil Dynamics and Earthquake Engineering, 2010. **30**(12): p. 1500-1512.
[15] Amado-Mendes, P., P. Alves Costa, L.M.C. Godinho and P. Lopes, *2.5D MFS–FEM model for the prediction of vibrations due to underground railway traffic.* Engineering Structures, 2015. **104**: p. 141-154.
[16] François, S., M. Schevenels, P. Galvín, G. Lombaert and G. Degrande, *A 2.5D coupled FE–BE methodology for the dynamic interaction between longitudinally invariant structures and a layered halfspace.* Computer Methods in Applied Mechanics and Engineering, 2010. **199**(23-24): p. 1536-1548.
[17] Jin, Q., D.J. Thompson, D.E.J. Lurcock, M.G.R. Toward and E. Ntotsios, *A 2.5D finite element and boundary element model for the ground vibration from trains in tunnels and validation using measurement data.* Journal of Sound and Vibration, 2018. **422**: p. 373-389.
[18] Yang, Y., H. Hung and H. Hsu, *Ground vibrations due to underground trains considering soil-tunnel interactions.* Interaction and Multiscale Mechanics, 2007. **1**(1): p. 157-175.
[19] Bian, X.C., W.F. Jin and H.G. Jiang, *Ground-borne vibrations due to dynamic loadings from moving trains in subway tunnels.* Journal of Zhejiang University: Science A, 2012. **13**(11): p. 870-876.
[20] Alves Costa, P., R. Calçada, J. Couto Marques and A. Cardoso, *A 2.5D finite element model for simulation of unbounded domains under dynamic loading*, in *7th European Conference on Numerical Methods in Geotechnical Engineering*, T. Benz and S. Nordal, Editors. 2010: Trondheim. p. 782-790.
[21] Yaseri, A., M.H. Bazyar and S. Javady, *2.5D coupled FEM-SBFEM analysis of ground vibrations induced by train movement.* Soil Dynamics and Earthquake Engineering, 2018. **104**: p. 307-318.
[22] François, S., M. Schevenels, G. Lombaert and G. Degrande, *A two-and-a-half-dimensional displacement-based PML for elastodynamic wave propagation.* International Journal for Numerical Methods in Engineering, 2012. **90**(7): p. 819-837.

[23] Lopes, P., P. Alves Costa, M. Ferraz, R. Calçada and A. Silva Cardoso, *Numerical modeling of vibrations induced by railway traffic in tunnels: From the source to the nearby buildings.* Soil Dynamics and Earthquake Engineering, 2014. **61-62**: p. 269-285.
[24] Lopes, P., J.F. Ruiz, P. Alves Costa, L. Medina Rodríguez and A.S. Cardoso, *Vibrations inside buildings due to subway railway traffic. Experimental validation of a comprehensive prediction model.* Science of The Total Environment, 2016. **568**: p. 1333-1343.
[25] Lopes, P., P. Alves Costa, R. Calçada and A. Silva Cardoso, *Influence of soil stiffness on vibrations inside buildings due to railway traffic: numerical study.* Computers & Geotechnics, 2014. **61**: p. 277-291.
[26] Castanheira-Pinto, A., P. Alves-Costa, L. Godinho and P. Amado-Mendes, *On the application of continuous buried periodic inclusions on the filtering of traffic vibrations: A numerical study.* Soil Dynamics and Earthquake Engineering, 2018. **113**: p. 391-405.
[27] Clouteau, D., M. Arnst, T. Al-Hussaini and G. Degrande, *Free field vibrations due to dynamic loading on a tunnel embedded in a stratified medium.* Journal of Sound and Vibration, 2005. **283**(1-2): p. 173-199.
[28] Gupta, S., Y. Stanus, G. Lombaert and G. Degrande, *Influence of tunnel and soil parameters on vibrations from underground railways.* Journal of Sound and Vibration, 2009. **327**: p. 70-91.
[29] Gupta, S., M. Hussein, G. Degrande, H. Hunt and D. Clouteau, *A comparison of two numerical models for the prediction of vibrations from underground railway traffic.* Soil Dynamics and Earthquake Engineering, 2007. **27**(7): p. 608-624.
[30] Gupta, S., G. Degrande and G. Lombaert, *Experimental validation of a numerical model for subway induced vibrations.* Journal of Sound and Vibration, 2009. **321**: p. 786-812.
[31] Gupta, S. and G. Degrande, *Modelling of continuous and discontinuous floating slab tracks in a tunnel using periodic approach.* Journal of Sound and Vibration, 2010. **329**(8): p. 1101-1025.
[32] Gupta, S., H. Berghe, G. Lombaert and G. Degrande, *Numerical modelling of vibrations from a Thalys high speed train in the Groene Hart tunnel* Soil Dynamics and Earthquake Engineering, 2010. **30**(3): p. 82-97.
[33] Hunt, H. and M. Hussein, *Vibration from railways: can we achieve better than +/- 10dB pridiction accuracy?*, in *ICSV14 - 14th International Congress on Sound and Vibration*. 2007: Cairns, Australia.
[34] Sadeghi, J., M.H. Esmaeili and M. Akbari, *Reliability of FTA general vibration assessment model in prediction of subway induced ground borne vibrations.* Soil Dynamics and Earthquake Engineering, 2019. **117**: p. 300-311.
[35] Mair, R. *Developments in geotechnical engineering research: application to tunnels and deep excavations.* in *Proceedings of the Institution of Civil Engineers-Civil Engineering*. 1993. Thomas Telford-ICE Virtual Library.
[36] Gomes, R.C., *Effect of stress disturbance induced by construction on the seismic response of shallow bored tunnels.* Computers and Geotechnics, 2013. **49**: p. 338-351.
[37] Duncan, J.M. and C.-Y. Chang, *Nonlinear analysis of stress and strain in soils.* Journal of Soil Mechanics Foundations Division, 1970.
[38] Schanz, T., P. Vermeer and P. Bonnier, *The hardening soil model: formulation and verification.* Beyond in computational geotechnics, 1999: p. 281-296.
[39] Benz, T., *Small-Strain Stiffness of Soils and its Numerical Consequences, Mitteilung des Instituts für Geotechnik der Universität Stuttgart*, in *Institut für Geotechnik*. 2006, Universität Stuttgart: Pfaffenwaldring. p. 209.
[40] Benz, T., *Small-strain stiffness of soils and its numerical consequences.* 2006, Institut für Geotechnik der Universität Stuttgart.
[41] Panet, M. and A. Guenot. *Analysis of convergence behind the face of a tunnel: Tunnelling 82, proceedings of the 3rd international symposium, Brighton, 7–11 June 1982, P197–*

204. Publ London: IMM, 1982. in *International Journal of Rock Mechanics and Mining Sciences & Geomechanics Abstracts*. 1983. Pergamon.

[42] Karakus, M. and R.J. Fowell, 2006., *2D and 3D finite element analyses for setllement due to soft ground tunnelling.*, in *Proceedings of the ITA-AITES 2006 World Tunnel Congress*. 2006.

[43] Deane, A.P. and R.H. Basset, *The Heathrow express trial tunnel.* Proc. Inst. Civil Engineers, 1995. **113**: p. 144.156.

[44] Callari, C. and S. Cassini, *Three-dimensional analysis of shallow tunnels in saturated soft ground.*, in *Proc. 5th Int. Symposium TC28 Geotechnical Aspects of Underground Construction in Soft Ground*, B. Bakker, Broere & Kwast Editor. 2006, Taylor & Francis/Balkema,. p. 495-501.

[45] Callari, C. and S. Cassini, *Tunnels in saturated elasto-plastic soils: three-dimensional validation of a plane simulation procedure.*, in *Mechanical Modelling and Computational Issues in Civil Engineering*, F. Maceri, Editor. 2005, Springer. p. 143-164.

[46] Topa Gomes, A., *Poços elípticos pelo método de escavação sequencial na vertical : o caso do Metro do Porto*, in *Faculty of Engineering*. 2008, University of Porto.

[47] Quagliata, A., M. Ahearn, E. Boeker, C. Roof, L. Meister and H. Singleton, *Transit Noise and Vibration Impact Assessment Manual*. 2018, Federal Transit Administration - Department of Transportation, Office of Planning and Environment. Washington DC.

[48] Hanson, C.E., J.C. Ross and D.A. Towers, *High-Speed Ground Transportation Noise and Vibration Impact Assessment*. 2012, Federal Railroad Administration - Department of Transportation, Office of Railroad Policy and Development. Washington DC.